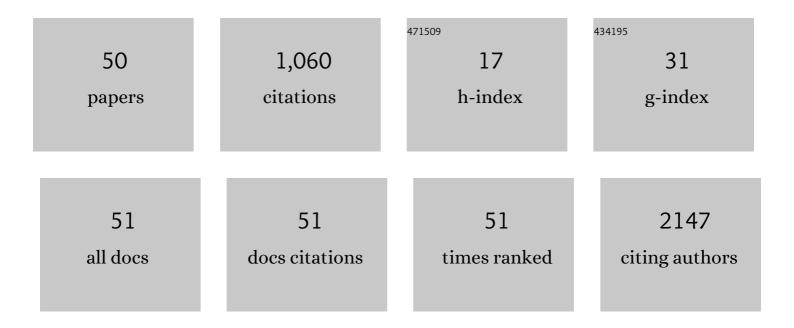
## **Benedicte Descamps**

List of Publications by Year in descending order

Source: https://exaly.com/author-pdf/1858672/publications.pdf Version: 2024-02-01



#	Article	IF	CITATIONS
1	Radiotherapy-Activated Cancer-Associated Fibroblasts Promote Tumor Progression through Paracrine IGF1R Activation. Cancer Research, 2018, 78, 659-670.	0.9	107
2	Sortase Aâ€mediated siteâ€specific labeling of camelid singleâ€domain antibodyâ€fragments: a versatile strategy for multiple molecular imaging modalities. Contrast Media and Molecular Imaging, 2016, 11, 328-339.	0.8	100
3	Co-delivery of nucleoside-modified mRNA and TLR agonists for cancer immunotherapy: Restoring the immunogenicity of immunosilent mRNA. Journal of Controlled Release, 2017, 266, 287-300.	9.9	98
4	Targeting of vascular cell adhesion molecule-1 by <sup>18</sup> F-labelled nanobodies for PET/CT imaging of inflamed atherosclerotic plaques. European Heart Journal Cardiovascular Imaging, 2016, 17, 1001-1008.	1.2	83
5	Pretreatment with VEGF(R)-inhibitors reduces interstitial fluid pressure, increases intraperitoneal chemotherapy drug penetration, and impedes tumor growth in a mouse colorectal carcinomatosis model. Oncotarget, 2015, 6, 29889-29900.	1.8	46
6	Radiation-induced lung damage promotes breast cancer lung-metastasis through CXCR4 signaling. Oncotarget, 2015, 6, 26615-26632.	1.8	39
7	A 3D CFD model of the interstitial fluid pressure and drug distribution in heterogeneous tumor nodules during intraperitoneal chemotherapy. Drug Delivery, 2019, 26, 404-415.	5.7	35
8	Tumor-environment biomimetics delay peritoneal metastasis formation by deceiving and redirecting disseminated cancer cells. Biomaterials, 2015, 54, 148-157.	11.4	34
9	Cx43 channels and signaling via IP3/Ca2+, ATP, and ROS/NO propagate radiation-induced DNA damage to non-irradiated brain microvascular endothelial cells. Cell Death and Disease, 2020, 11, 194.	6.3	34
10	MRI-guided 3D conformal arc micro-irradiation of a F98 glioblastoma rat model using the Small Animal Radiation Research Platform (SARRP). Journal of Neuro-Oncology, 2014, 120, 257-266.	2.9	32
11	Haematopoietic prolyl hydroxylaseâ€1 deficiency promotes M2 macrophage polarization and is both necessary and sufficient to protect against experimental colitis. Journal of Pathology, 2017, 241, 547-558.	4.5	32
12	18F-fluoromethylcholine (FCho), 18F-fluoroethyltyrosine (FET), and 18F-fluorodeoxyglucose (FDG) for the discrimination between high-grade glioma and radiation necrosis in rats: A PET study. Nuclear Medicine and Biology, 2015, 42, 38-45.	0.6	30
13	Preclinical evaluation of local prolonged release of paclitaxel from gelatin microspheres for the prevention of recurrence of peritoneal carcinomatosis in advanced ovarian cancer. Scientific Reports, 2019, 9, 14881.	3.3	25
14	Dynamic changes in hippocampal diffusion and kurtosis metrics following experimental mTBI correlate with glial reactivity. NeuroImage: Clinical, 2019, 21, 101669.	2.7	25
15	Can medical imaging identify the histopathological growth patterns of liver metastases?. Seminars in Cancer Biology, 2021, 71, 33-41.	9.6	23
16	Hypoxia imaging with 18F-FAZA PET/CT predicts radiotherapy response in esophageal adenocarcinoma xenografts. Radiation Oncology, 2018, 13, 39.	2.7	22
17	Alterations in the functional brain network in a rat model of epileptogenesis: A longitudinal resting state fMRI study. NeuroImage, 2019, 202, 116144.	4.2	22
18	Synergy between Intraperitoneal Aerosolization (PIPAC) and Cancer Nanomedicine: Cisplatin-Loaded Polyarginine-Hyaluronic Acid Nanocarriers Efficiently Eradicate Peritoneal Metastasis of Advanced Human Ovarian Cancer. ACS Applied Materials & Interfaces, 2020, 12, 29024-29036.	8.0	19

BENEDICTE DESCAMPS

#	Article	IF	CITATIONS
19	New fluoroethyl phenylalanine analogues as potential LAT1-targeting PET tracers for glioblastoma. Scientific Reports, 2019, 9, 2878.	3.3	18
20	Dynamic functional connectivity and graph theory metrics in a rat model of temporal lobe epilepsy reveal a preference for brain states with a lower functional connectivity, segregation and integration. Neurobiology of Disease, 2020, 139, 104808.	4.4	18
21	Kinetic Modeling and Graphical Analysis of 18F-Fluoromethylcholine (FCho), 18F-Fluoroethyltyrosine (FET) and 18F-Fluorodeoxyglucose (FDG) PET for the Fiscrimination between High-Grade Glioma and Radiation Necrosis in Rats. PLoS ONE, 2016, 11, e0161845.	2.5	17
22	Biocompatible Lipidâ€Coated Persistent Luminescent Nanoparticles for In Vivo Imaging of Dendritic Cell Migration. Particle and Particle Systems Characterization, 2019, 36, 1900371.	2.3	16
23	Adjuvant therapeutic potential of tonabersat in the standard treatment of glioblastoma: AÂpreclinical F98 glioblastoma rat model study. PLoS ONE, 2019, 14, e0224130.	2.5	16
24	In Vivo DCE-MRI for the Discrimination Between Glioblastoma and Radiation Necrosis in Rats. Molecular Imaging and Biology, 2017, 19, 857-866.	2.6	15
25	Performance evaluation of the LightPath imaging system for intra-operative Cerenkov luminescence imaging. Physica Medica, 2018, 52, 122-128.	0.7	13
26	The shrimp nephrocomplex serves as a major portal of pathogen entry and is involved in the molting process. Proceedings of the National Academy of Sciences of the United States of America, 2020, 117, 28374-28383.	7.1	13
27	Intra-individual dynamic comparison of 18F-PSMA-11 and 68Ga-PSMA-11 in LNCaP xenograft bearing mice. Scientific Reports, 2020, 10, 21068.	3.3	12
28	The Path Toward PET-Guided Radiation Therapy for Glioblastoma in Laboratory Animals: A Mini Review. Frontiers in Medicine, 2019, 6, 5.	2.6	11
29	Exploratory relationships between cognitive improvements and training induced plasticity in hippocampus and cingulum in a rat model of mild traumatic brain injury: a diffusion MRI study. Brain Imaging and Behavior, 2020, 14, 2281-2294.	2.1	10
30	2-[18F]FELP, a novel LAT1-specific PET tracer, for the discrimination between glioblastoma, radiation necrosis and inflammation. Nuclear Medicine and Biology, 2020, 82-83, 9-16.	0.6	10
31	Technical feasibility of [18F]FET and [18F]FAZA PET guided radiotherapy in a F98 glioblastoma rat model. Radiation Oncology, 2019, 14, 89.	2.7	9
32	Development of a Rat Model for Glioma-Related Epilepsy. International Journal of Molecular Sciences, 2020, 21, 6999.	4.1	8
33	Species-dependent extracranial manifestations of a brain seeking breast cancer cell line. PLoS ONE, 2018, 13, e0208340.	2.5	7
34	Impact of the molar activity and PSMA expression level on [18F]AlF-PSMA-11 uptake in prostate cancer. Scientific Reports, 2021, 11, 22623.	3.3	7
35	PET and MRI Guided Irradiation of a Glioblastoma Rat Model Using a Micro-irradiator. Journal of Visualized Experiments, 2017, , .	0.3	6
36	Cytosolic delivery of gadolinium <i>via</i> photoporation enables improved <i>in vivo</i> magnetic resonance imaging of cancer cells. Biomaterials Science, 2021, 9, 4005-4018.	5.4	6

#	Article	IF	CITATIONS
37	Radiosynthesis, in vitro and preliminary in vivo evaluation of the novel glutamine derived PET tracers [18F]fluorophenylglutamine and [18F]fluorobiphenylglutamine. Nuclear Medicine and Biology, 2020, 86-87, 20-29.	0.6	5
38	Slc2a10 knock-out mice deficient in ascorbic acid synthesis recapitulate aspects of arterial tortuosity syndrome and display mitochondrial respiration defects. Human Molecular Genetics, 2020, 29, 1476-1488.	2.9	5
39	Assessment of the effect of therapy in a rat model of glioblastoma using [18F]FDG and [18F]FCho PET compared to contrast-enhanced MRI. PLoS ONE, 2021, 16, e0248193.	2.5	5
40	In vivo selection of the MDA-MB-231br/eGFP cancer cell line to obtain a clinically relevant rat model for triple negative breast cancer brain metastasis. PLoS ONE, 2020, 15, e0243156.	2.5	5
41	Voxel-Based Analysis of [18F]-FDG Brain PET in Rats Using Data-Driven Normalization. Frontiers in Medicine, 2021, 8, 744157.	2.6	5
42	Quantitative and Functional Requirements for Bioluminescent Cancer Models. In Vivo, 2016, 30, 1-11.	1.3	4
43	Improved xenograft efficiency of esophageal adenocarcinoma cell lines through in vivo selection. Oncology Reports, 2017, 38, 71-81.	2.6	3
44	Advanced Diffusion Imaging in The Hippocampus of Rats with Mild Traumatic Brain Injury. Journal of Visualized Experiments, 2019, , .	0.3	3
45	Radiosynthesis, in vitro and preliminary biological evaluation of [ <sup>18</sup> F]2â€aminoâ€4â€{(2â€{(3â€fluorobenzyl)oxy)benzyl)(2â€{(3â€{fluoromethyl)benzyl)oxy)benzyl) acid, a novel alanine serine cysteine transporter 2 inhibitorâ€based positron emission tomography tracer. lournal of Labelled Compounds and Radiopharmaceuticals. 2020. 63. 442-455.	vl)amino)t 1.0	outanoic
46	In Vivo Electrical Conductivity Imaging of Animal Tumor Model at 7T using Electrical Properties Tomography. , 2018, , .		1
47	Comparison of In Vivo and Ex Vivo Magnetic Resonance Imaging in a Rat Model for Glioblastoma-Associated Epilepsy. Diagnostics, 2021, 11, 1311.	2.6	1
48	White Matter Integrity in a Rat Model of Epileptogenesis: Structural Connectomics and Fixel-Based Analysis. Brain Connectivity, 2022, 12, 320-333.	1.7	1
49	Evaluation of Liposome-Loaded Microbubbles as a Theranostic Tool in a Murine Collagen-Induced Arthritis Model. Scientia Pharmaceutica, 2022, 90, 17.	2.0	1
50	Positron Emission Tomography-based Dose Painting Radiation Therapy in a Clioblastoma Rat Model using the Small Animal Radiation Research Platform. Journal of Visualized Experiments, 2022, , .	0.3	0